Catal Lett (2007) 118:264–269
DOI 10.1007/s10562-007-9182-x

A Cu/Zn/Al/Zr Fibrous Catalyst that is an Improved CO_2 Hydrogenation to Methanol Catalyst

Xin An · Jinlu Li · Yizan Zuo · Qiang Zhang · Dezheng Wang · Jinfu Wang

Received: 1 May 2007 / Accepted: 20 June 2007 / Published online: 17 July 2007
© Springer Science+Business Media, LLC 2007

Abstract A series of Cu/Zn/Al/Zr CO_2 hydrogenation to methanol catalysts containing different ratios of Al/Zr were prepared using a co-precipitation procedure. SEM, TEM, and XRD characterization showed that all the catalysts comprised crystallites in a fibrous structure and their Cu/Zn crystallite dispersions were better than that of a commercial (COM) catalyst. It is suggested that the high dispersion and stability of the Cu/Zn crystallites due to the fibrous structure enhanced CO_2 hydrogenation, and the added Zr component further improved the catalyst. A 5% Zr addition gave a methanol space time yield 80% higher than that on the COM catalyst.

Keywords Cu/Zn/Al/Zr · CO_2 hydrogenation

1 Introduction

The greenhouse effect is a threat to the living environment of mankind. The conversion of CO_2 that would otherwise get into the atmosphere into useful chemicals, e.g. methanol, is an attractive way to protect the global environment since CO_2 is an important greenhouse gas and methanol itself is a useful raw chemical and solvent. For CO_2 hydrogenation, the thermodynamics analysis showed that when the reaction temperature is increased, CO_2 conversion is slightly decreased and methanol selectivity is decreased, so that the yield of methanol is decreased [1, 2]. An industrial CO_2 hydrogenation process should be operated at a relative low reaction temperature. However, a conventional Cu/Zn/Al catalyst that is active for methanol production from synthesis gas (mixture of CO, CO_2, and H_2 [3]) is not as active and selective for methanol synthesis from a H_2/CO_2 mixture at temperatures below 250 °C [4–13], even though it is now accepted that methanol synthesis from synthesis gas actually proceeds through CO_2 hydrogenation. For CO_2 conversion to methanol, there is still the need to develop a highly active and stable catalyst.

Several modifications have been used to improve conventional Cu/Zn/Al methanol synthesis catalysts. The key is to keep a high dispersion of the Cu/Zn crystallites where the active sites are [7–19]. Some works seek to improve the dispersion of the conventional Cu/Zn/Al catalyst by using complicated preparation procedure or expensive organic solvents. Other works seek to improve the catalyst by adding additives other than Al to Cu/Zn crystallites or Cu/Zn/Al composites, e.g., Melian-Cabrera, Granados and Fierro [7–11] reported the use of Cr, Zr, V, Ce, Ti, Ga, and Pd to modify Cu/ZnO-based catalysts. Some additives, such as Ce, Ga, Pd, are quite expensive. The increase in catalytic activity was limited. There are few reports on catalyst morphology control, which is also an important aspect for a high performance catalyst. Recently, we found that the catalyst performance can be enhanced by the control of the catalyst structure [19, 20]. For example, by using a well controlled coprecipitation procedure, a Cu/Zn/Al catalyst with a fibrous structure with high activity and thermal stability for both CO and CO_2 hydrogenation was developed [18]. The fibrous structure gave the catalysts a higher specific surface area and at the same time restrained Cu/Zn crystallites from sintering, which enhanced the CO_2 hydrogenation. In addition to morphology control, the

X. An · J. Li · Y. Zuo · Q. Zhang · D. Wang · J. Wang (✉)
Beijing Key Laboratory of Green Chemical Reaction Engineering and Technology, Department of Chemical Engineering, Tsinghua University, Beijing 100084, China
e-mail: wangjf@flotu.org

adding of another element may also improve the catalyst performance further [20].

In this work, we began with a fibrous Cu/Zn/Al catalyst and studied a new catalyst obtained by Zr addition substituting all or a part of Al. The Cu/Zn/Al/Zr catalysts also had the fibrous structure. Both the added Zr component and fibrous morphology had good effects on catalytic activity.

2 Experimental

Five catalysts, CD401–CD405 were prepared by using a novel co-precipitation procedure reported in An et al. [19]. The catalysts were prepared using the corresponding nitrates as the metal sources and sodium carbonate as the precipitant. The precipitate was washed, dried, and calcined at 350 °C for 4 h to yield the Cu/Zn/Al/Zr catalyst. CD401 was a Cu/Zn/Al (without Zr) catalyst with quite high activity and stability. CD402–CD404 were Cu/Zn/Al/Zr catalysts with added Zr present in different Al/Zr ratios, in which the sum of the contents of Al and Zr was constant and equal to 10 mole%. CD405 was a Cu/Zn/Zr catalyst (without Al). The composition and specific surface area of CD401–405 are shown in Table 1. As a reference catalyst, a commercial catalyst codenamed COM that had been successfully used in many plants in China for producing methanol from synthesis gas was used. There have been many generations of commercial catalysts for methanol synthesis, and this is perhaps the most commonly used industrial catalyst in China at present.

The activity tests were carried out in a fixed bed reactor. Before reaction, the catalyst was reduced with a 5%H_2/95%N_2 mixture at atmospheric pressure by raising the temperature slowly to the reaction temperature over 10 h. Then the reduction gas was switched to the reaction gas and the pressure was raised to the reaction pressure to start the reaction. The first sample of the effluent was taken 2 h after steady reaction conditions were established, and then samples were taken every 30 min for online analysis of the effluent composition by a gas chromatograph. The final result used is an average of five data points. To examine the thermal stability of the catalyst, an overheating test was done on each catalyst in the following way: after 4 h of reaction under the normal reaction conditions, the reaction temperature was raised to 400 °C and the reaction was conducted at this temperature for 3 h with other conditions unchanged, and then the temperature was brought down to the original temperature to determine the activity of the catalyst.

The morphology of the catalyst before reaction was characterized by high resolution scanning electron microscopy (HRSEM, JSM 7401F, at 5.0 kV) and high resolution transmission electron microscopy (HRTEM, JEM 2010, at 200.0 kV). Powder X-ray diffraction (XRD) patterns of the catalysts were obtained with a BRUKER D8 Advance type X-ray diffractometer using nickel-filtered Cu Kα radiation. The patterns were recorded for $10^\circ < 2\theta < 90^\circ$. The BET surface area was obtained with a high resolution BET equipment described in Wang et al. [21, 22].

3 Results and Discussion

The morphologies of the powder Cu/Zn/Al/Zr catalysts CD401–CD405 characterized by SEM are shown in Fig. 1. All the Cu/Zn/Al/Zr catalyst existed as regular one-dimensional nanomaterial agglomerates. The Al/Zr ratio had a clear influence on the morphology. Catalysts CD401–CD404, whose Zr contents increased gradually, all had the fibrous structure in which the crystallites were assembled into thin nm-diameter fibers (Fig. 1a–d). The fiber diameters were uniformly distributed, and averaged 25 nm, 18 nm, 14 nm, and 18 nm, respectively. All of the length to diameter ratio were higher than 20. Catalyst CD405, which was Cu/Zn/Zr, was mainly plate-like microcrystals, whose minimum dimension was about 70 nm. The CD403 catalyst had the smallest diameter, which indicated it is potentially the best catalyst. Thus, in contrast to the COM catalyst, which consisted of irregular particles of about 30 nm that exist in much larger and diverse agglomerates, a catalyst with a one-dimensional fibrous structure was obtained with our catalyst preparation strategy.

Table 1 Composition of the Cu/Zn/Al/Zr catalysts for CO_2 hydrogenation to methanol

Catalyst	Composition of catalyst				Surface area ($m^2 \cdot g^{-1}$)
	Cu (mol%)	Zn (mol%)	Al (mol%)	Zr (mol%)	
CD401	60	30	10.0	0.0	68.8
CD402	60	30	7.5	2.5	69.9
CD403	60	30	5.0	5.0	70.9
CD404	60	30	2.5	7.5	69.7
CD405	60	30	0.0	10.0	64.2
COM	–	–	–	–	54.6

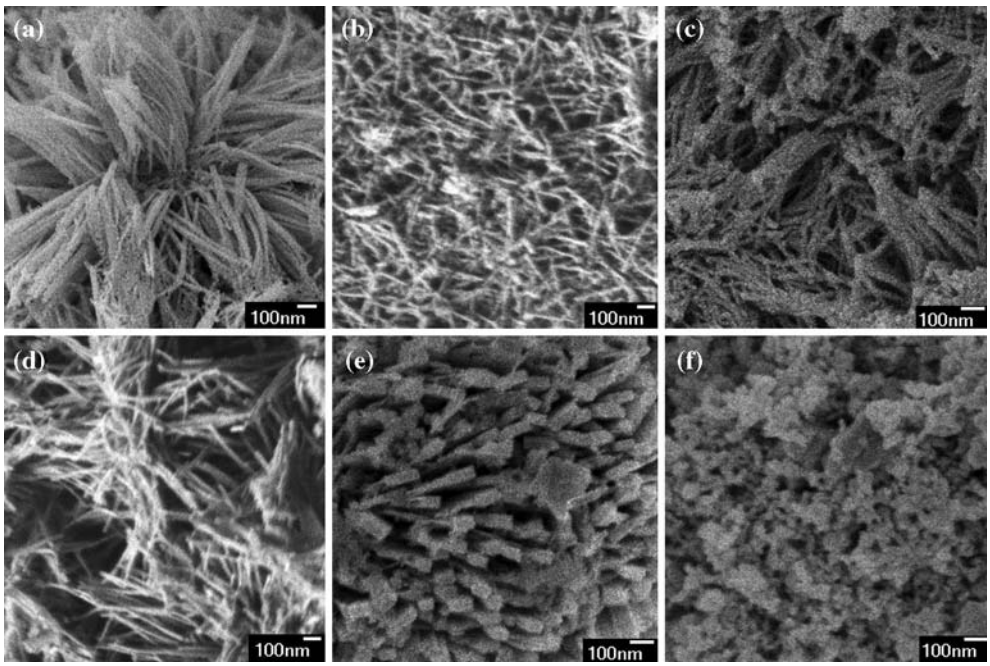

Fig. 1 Morphology of the Cu/Zn/Al/Zr catalysts before reaction: (**a**) CD401; (**b**) CD402; (**c**) CD403; (**d**) CD404; (**e**) CD405; (**f**) COM

The detailed morphology of the Cu/Zn/Al/Zr catalysts is shown in the high magnification TEM images in Fig. 2, in which the fibrous morphology is also seen. All the catalysts consisted of nanoparticles that agglomerated into nm-diameter fibers or platelike microcrystals by self assembly, which might be related to the presence of ZnO. This needs further study. It was difficult to acquire the high resolution TEM images due to the poor crystallinity, which was confirmed by the XRD results (see below). These TEM images also indicated that the CD403 catalyst had the thinnest rods.

The XRD patterns that characterized the structure of the Cu/Zn/Al/Zr catalysts are shown for CD401, CD403, CD405, and COM in Fig. 3 (the XRD patterns of CD402 and CD404 were similar to those of CD401 and CD403, and are omitted from the figure). The poor crystallinity of the catalysts is shown by the low signal-noise ratio. Only a few peaks can be seen above the baseline. In the XRD patterns of CD401–CD404, there were only rather weak peaks that can be assigned to CuO, which was the main component of the Cu/Zn/Al/Zr catalyst. These appeared at $2\theta = 35.5°$ ($d = 2.520$Å), 38.6° (d = 2.327 Å), and 48.8° (d = 1.870Å). There were no peaks that can be assigned to ZnO, Al_2O_3, and ZrO_2, indicating that ZnO, Al_2O_3, and ZrO_2 existed in an amorphous or microcrystalline state. In addition to the above three peaks, in the XRD patterns of CD405 and COM there also appeared peaks that were assigned to ZnO at $2\theta = 31.8°$ (d = 2.809 Å), 34.3° (d = 2.599 Å), 36.2° (d = 2.486 Å), 47.4° (d = 1.906 Å), 56.6° (d = 1.626 Å), 62.8° (d = 1.477 Å), and 67.8° (d = 1.378 Å). A peak at 26.5° (d = 3.35 Å) in the XRD pattern of COM was assigned to $(Cu,Zn)_6(AlOH)_{16}CO_3 \cdot 4H_2O$ [23]. The identification of the peaks agreed well with that by Wu and Xiao [23] and Yang et al. [24]. The structure has a close relationship with the catalyst behavior, as will be discussed.

The thermodynamics of methanol synthesis by CO_2 hydrogenation based on Reid's thermodynamic data and the Soave–Redlich–Kwong equation of state was calculated for the same conditions as the experiments [2]. This is

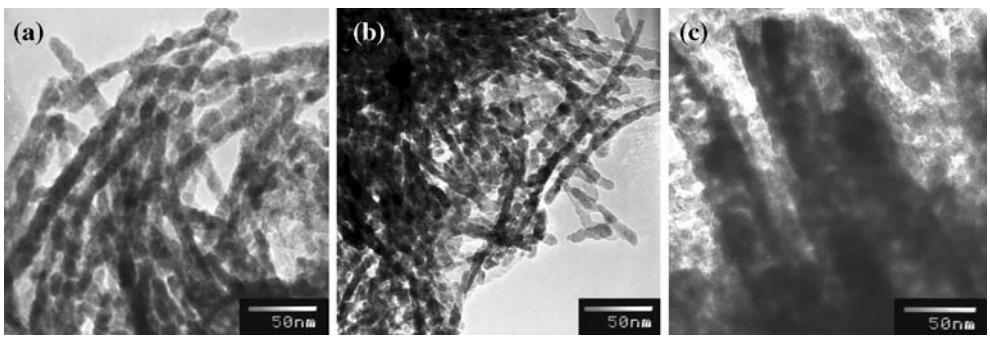

Fig. 2 TEM images of the Cu/Zn/Al/Zr catalysts before reaction: (**a**) CD401; (**b**) CD403; (**c**) CD405

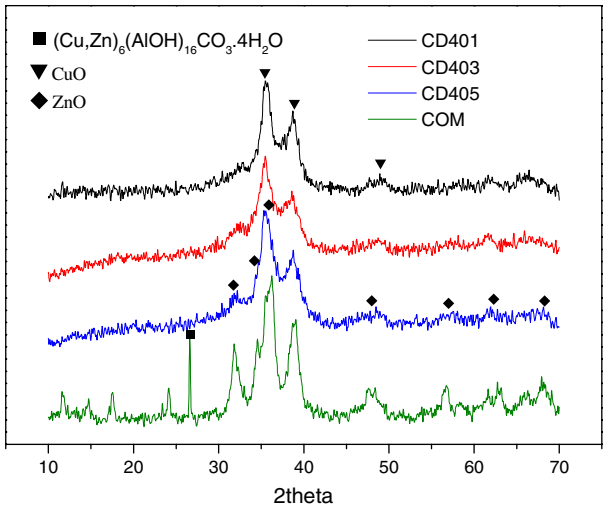

Fig. 3 XRD patterns of the Cu/Zn based catalysts

shown and compared with the experimental catalyst activity for CO_2 hydrogenation in Fig. 4. The thermodynamics is such that both CO_2 conversion and methanol selectivity were lower at a higher reaction temperature. Experimentally, the CO_2 conversion increased with temperature for CD403, and approached the thermodynamic limit above 250 °C. Experimentally, the methanol selectivity increased slightly and then decreased with temperature, and also gradually reached the thermodynamics limit. At 240 °C, both the CO_2 conversion and the methanol selectivity were relatively high, and not too close to the thermodynamic limit. Thus, 240 °C was used to compare the catalytic activity of the Cu/Zn/Al/Zr catalysts and the commercial catalyst, COM. The results are listed in Table 2.

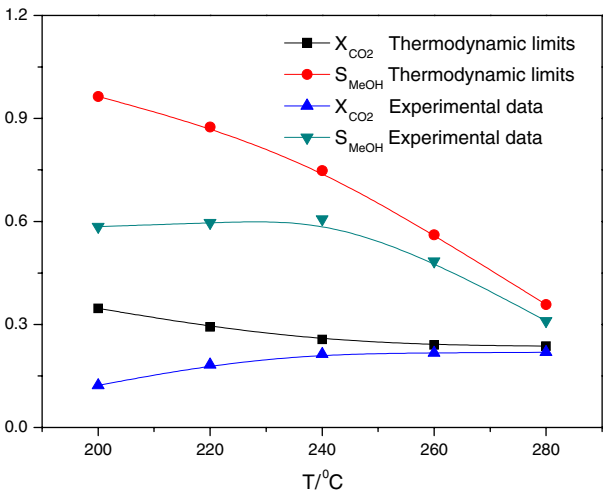

Fig. 4 Thermodynamic limits and experimental relationship between CO_2 conversion, methanol selectivity and reaction temperature for CD403 catalyst

The CO_2 conversions of the Cu/Zn/Al/Zr catalysts were higher, by at least 17% more, than the COM catalyst. The selectivity to methanol was increased at least 18% compared with the COM catalyst. The methanol space time yields (STYs) were increased 35%. The sum of the selectivity to methanol and CO was 100% since the other products were negligible under the mild conditions. The data indicated that the Cu/Zn/Al/Zr catalysts showed much better activity and methanol selectivity than the commercial industrial catalyst for CO_2 conversion.

The catalyst functions of the Al and Zr contents were studied. CO_2 conversion, methanol selectivity, and methanol STY first increased with an increase of the Zr content, then decreased. The methanol STY on the catalyst modified with 5 mole% Al plus 5 mole% Zr (CD403) was 81% higher than that on the industrial catalyst (COM), 11% higher than that on the catalyst with only Al (CD401), and 31% higher than that on the catalyst modified with only ZrO_2 (CD405). The methanol selectivity of CD403 was 43% higher than that on COM, 9.1% higher than that on CD401, and 11% higher than that on CD405. These data clearly demonstrated that CD403 was the best catalyst for CO_2 hydrogenation to methanol.

The catalyst stability was also closely related to the dispersion of the Cu/Zn crystallites. Most researchers believe that Cu easily sinters to give a poor dispersion of the Cu/Zn crystallites [25–29], and this is a most important factor in catalyst activity loss. The high temperature treatment was a demanding atmosphere for the Cu/Zn/Al/Zr catalyst, and the overheating experiment was a test of the stability of the catalysts. After overheating, even better catalyst behaviors were shown as compared with COM. The trends versus the content of ZrO_2 in the variations in CO_2 conversion, methanol selectivity, CO selectivity, and methanol STY were the same as before overheating, but the extents of the variations were larger. For example, the STY of methanol on the catalyst CD403 was 28% higher (before overheating, this was 5%) than that on the catalyst CD401 (modified with only Al_2O_3), and 106% higher (before overheating, this was 11%) than that on the catalyst CD405 (modified with only ZrO_2). These data demonstrated that the synergetic effect from the additives was more after overheating. In addition, methanol STY over CD401 and CD405, especially CD 405, decreased more after overheating than was the case with CD403. The methanol STY over CD401 and CD 405 dropped by 63% and 108%, respectively, while that over CD 403 decreased only by 41%, indicating that the modification of the catalyst with Al_2O_3 plus ZrO_2, not only can enhance the activity of the catalyst, but also enhance the thermal stability. Moreover, the improvement of the activity may also prolong the catalyst lifetime because the reaction temperature can be lowered for the same productivity of methanol

Table 2 Catalytic activity of the catalysts modified by Al_2O_3 and/or ZrO_2

Catalyst No.	CO_2 conversion (%)		MeOH selectivity (%)		CO selectivity (%)		MeOH STY ($g \cdot mL^{-1} \cdot h^{-1}$)	
	BO[b]	AO[c]	BO	AO	BO	AO	BO	AO
CD401	20.09	17.64	55.93	39.14	44.07	60.86	0.3910	0.2403
CD402	20.49	19.04	58.35	45.29	41.65	54.71	0.4160	0.3000
CD403	20.51	18.79	61.01	47.24	38.99	52.76	0.4352	0.3082
CD404	20.29	18.43	58.45	44.16	41.55	55.84	0.4126	0.2832
CD405	19.02	14.21	50.31	30.28	49.69	69.72	0.3330	0.1498
COM	16.25	11.46	42.61	45.62	57.39	54.38	0.2406	0.1819

[a] Reaction conditions: T = 240 °C, p = 4.0 MPa, Sv = 9742 h^{-1}, Feed gas: H_2:CO_2 = 3:1

[b] Before overheating

[c] After overheating

and the lowering of the temperature avoids the sintering of Cu.

The stability of the yield of methanol from CO_2 hydrogenation with CD403 was also tested at 230 °C and a space velocity of 3000 ml/(g h). The results are shown in Fig. 5. In the first 24 h, the methanol yield decreased from 14.4% to 13.0%, then was constant at 13% for nearly 300 h. The stability seen on CD403 was high.

Compared to the commercial catalyst (COM), CD403 had a much higher STY before and after overheating. The STY of CD403 was high enough under mild conditions that both the activity and stability of CD403 can be considered to have reached practical value.

It is commonly believed that the active site for CO_2 hydrogenation to methanol is on the Cu/Zn crystallites [18, 26]. A high dispersion of the Cu/Zn crystallites during the

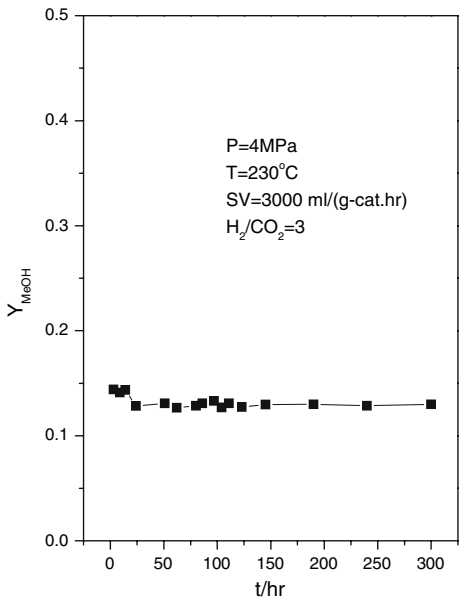

Fig. 5 Stability of the CD403 catalyst as shown by the yield of methanol from CO_2 hydrogenation

catalyst lifetime is one of the most effective ways to improve catalyst activity. There are two important factors. First, the Cu/Zn crystallites must be initially well dispersed on the catalyst. The XRD patterns of CD405 and COM contained many peaks of ZnO, but these peaks did not appear in the XRD patterns of CD401–CD404, which indicated that CD405 and COM contained larger crystallites of ZnO. The particle size of the ZnO in CD401–CD404 was much smaller. There is also a possibility that ZnO is dispersed in the CuO matrix, which would result in less intimate contact between the Cu and ZnO active components in CD401–CD404 than in CD405 and COM. However, on comparing the XRD peaks that were assigned to CuO, that of CD403 had a half width that was wider than that of CD401, CD402, and CD404. This means that the CuO crystallite size in CD403 was the smallest among all the catalysts studied, and it can be recalled that CD403 showed the best catalytic behavior.

The second factor for the high activity of a Cu/Zn/Al/Zr catalyst is related to the effect of ion doping and valence compensation. Zr^{4+} dissolved in the ZnO crystal causes the formation of positive ion defects on the surface of Cu–ZnO. These defects can adsorb Cu^+ and form and stabilize more active sites, Cu^0-Cu^+-O-Zn^{2+}, on the catalyst surface [12] Fig. 6.

A better dispersion of Cu/Zn crystallites was obtained with the proper addition of the fourth element (Zr). In addition, catalyst sintering was effectively inhibited because the catalyst existed in a more suitable (fibrous) morphology, which was also a key factor. The controlling of the catalyst morphology was an effective way to achieve this. In the COM catalyst, the catalyst particle existed as agglomerates of particles that had a surface area of 54.6 m^2/g. In contrast, the fibrous Cu/Zn/Al/Zr catalysts had higher surface areas. The surface areas of CD401–CD405 are shown in Table 1. These catalysts were discrete fibrous rods, as shown in Fig. 1 and 2. The fibrous catalysts with high surface areas were better catalysts as shown in

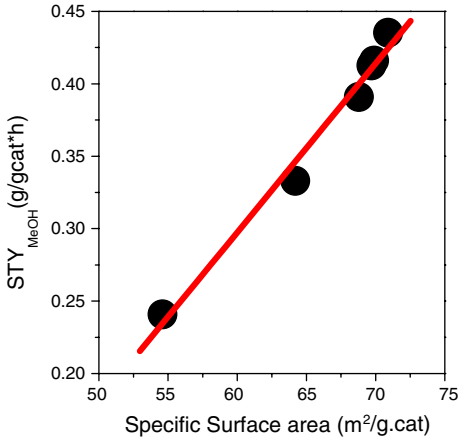

Fig. 6 Relationship between the methanol STY and specific surface area of the Cu/Zn based catalysts

Fig. 4, which shows a linear relationship between the methanol STY and the surface area.

In addition, in the fibrous catalyst, it can be inferred that most of the nanoparticles had easier movement in the axial direction of the fiber. Movement in the radial direction would be less facile, which is evident from the small diameter of the fiber, which is not the case with the particle aggregate catalyst morphology of COM. Cu or Zn must diffuse along the single fiber-like structure, which will make catalyst sintering much more difficult. Even after a high temperature treatment to induce sintering, the CD403 catalyst also showed the highest STY, which was much better than that of the COM catalyst. This showed that the stability of the catalyst was also better during severe heat treatment. Besides, in the COM catalyst, the presence of undecomposed $(Cu,Zn)_6(AlOH)_{16}CO_3 \cdot 4H_2O$ in COM after calcination may be another reason for the lower activity of COM. $(Cu,Zn)_6(AlOH)_{16}CO_3 \cdot 4H_2O$ does not decompose when the reduction and reaction were performed at a temperature lower than the calcination temperature and it is not an active component.

4 Conclusions

A better CO_2 hydrogenation to methanol Cu/Zn/Al/Zr catalyst was obtained by promoter addition and morphology control by Zr and Al addition, and the catalyst preparation method. Both the activity and the methanol selectivity of CO_2 hydrogenation were improved. A better dispersion of the Cu/Zn crystallites and the fibrous structure of the catalyst were the main factors for the higher activity and stability. Catalyst CD403, with 5 mole% Zr showed the best activity and thermal stability with a methanol STY that was 81% higher than a commercial industrial catalyst. The catalyst performance enhancement was achieved with component control and morphology control.

Acknowledgments The authors gratefully acknowledge the financial supports by the Chinese National Science Foundation (nos. 20576060, 20606021), and by Specialized Research Fund for the Doctoral Program of Higher Education (no. 20050003030).

References

1. Skrzypek J, Lachowska M, Grzesik M, Sloczynski J, Nowak P (1995) Chem Eng J Biochem Eng J 58:101
2. An X, Li JL, Wang JF (2007) Natural Gas Chem Ind (in press)
3. Lange J-P (2001) Catal Today 64:3
4. Liu XM, Lu GQ, Yan ZF (2003) Ind Eng Chem Res 42:6518
5. Zhilyaeva NA, Volnina EA, Kukina MA (2002) Petrol Chem 42:367
6. Saito M, Takeuchi M, Watanabe T, Toyir J, Luo SC, Wu JG (1997) Engergy Convers Magn 38:403
7. Melian-Cabrera I, Granados ML, Fierro JLG (2002) J Catal 210:273
8. Melian-Cabrera I, Granados ML, Fierro JLG (2002) J Catal 210:285
9. Melian-Cabrera I, Granados ML, Fierro JLG (2002) Catal Lett 79:165
10. Melian-Cabrera I, Lopez Granados M, Terreros P, Fierro JLG (1998) Catal Today 45:251
11. Melian-Cabrera I, Granados ML, Fierro JLG (2002) Catal Lett 84:153
12. Lin RC, Yang YQ, Yuan YZ, Lin ZY, Li C, Yang H, Wang Q, Zhang HB (2001) J Natural Gas Chem 10:308
13. Cao Y, Chen LF, Dai WL, Fan KN, Wu D, Sun YH (2003) Chem J Chinese U 24:1296
14. Busca G, Costantino U, Marmottini F, Montanari T, Patrono P, Pinzari F, Ramis G (2006) Appl Catal A 310:70
15. Wang J, Funk S, Burghaus U (2005) Catal Lett 103:219
16. Schuyten S, Wolf EE (2006) Catal Lett 106:7
17. Zhang XR, Wang LC, Yao CZ, Cao Y, Dai WL, He HY, Fan KN (2005) Catal Lett 102:183
18. Ostrovskii VE (2002) Catal Today 77:141
19. An X, Ren F, Li JL, Wang JF (2005) Chinese J Catal 26:729
20. Zhang Q, Qian WZ, Wen Q, Liu Y, Wang DZ, Wei F (2007) Carbon (doi:10.1016/j.carbon.2007.03.045)
21. Wang DZ, Wei F, Wang JF (2006) US patent 6,981,426 (Jan, 2006)
22. Li FX, Wang Y, Wang DZ, Wei F (2004) Carbon 42:2375
23. Wu SC, Xiao SY (1994) Petrochem Tech 23:37
24. Yang YQ, Zhang HB, Lin GD, Chen HZ, Yuan YZ, Tsa KR (1994) J Shamen Univ 33:477
25. Wu JG, Saito M, Takeuchi M, Watanabe T (2001) Appl Catal A 218:235
26. Pillai UR, Deevi S (2006) Appl Catal A 65:110
27. Aguayo AT, Erena J, Sierra I, Olazar M, Bilbao J (2005) Catal Today 106:265
28. Denise B, Sneeden RPA (1986) Appl Catal 28:235
29. Saito M, Wu JG, Tomoda K, Takahara I, Murata K (2002) Catal Lett 83:1